Biosensors and Bioelectronics 26 (2011) 4308–4313

Contents lists available at ScienceDirect

Biosensors and Bioelectronics

journal homepage: www.elsevier.com/locate/bios

Silver nanoparticles as redox reporters for the amplified electrochemical detection of the single base mismatches

Masoud A. Mehrgardi*, Laleh Enayati Ahangar

Department of chemistry, Faculty of science, University of Isfahan, Isfahan 81746-73441, Iran

ARTICLE INFO

Article history:
Received 1 February 2011
Received in revised form 9 April 2011
Accepted 11 April 2011
Available online 16 April 2011

Keywords:
DNA hybridization biosensor
Thermodynamically stable mismatches
Silver nanoparticles
Charge transfer in DNA

ABSTRACT

In this manuscript, a strategy for the amplification of the responses of an electrochemical DNA hybridization biosensor using silver nanoparticles (Ag-NPs) as redox reporters and its capability for the detection of a single base mismatches (SBM) including thermodynamically stable ones, is described. In this assay, Ag-NPs are immobilized on the top of recognition layer and their oxidation signals are followed. Differential pulse voltammetry (DPV) and electrochemical impedance spectroscopy (EIS) are used to monitoring the electrode response. Only for complementary target sequence, electron can transfer between Electrode surface and nanoparticles via DNA and Ag-NPs can be oxidized. Therefore this DNA biosensor could differentiate between complementary target and one containing either SBM or thermodynamically stable G–A and G–T targets through oxidation signal of Ag-NPs. This biosensor is able to detect SBM by overcome the direct electron transfer of redox reporter with electrode surface and positioning of it before the mismatch position.

1. Introduction

One of the important applications of DNA biosensors is investigation of genetic disorders. Identification of mutation in nucleic acids is an important part of genetic research, not at least for the prediction and diagnosis of diseases and their medical treatments (Li et al., 2009; Steel et al., 1998). Detection of a single base mismatch is very important for the perception genetic mutation. Several methods have been developed to detect SBMs, such as fluorescence (Niu et al., 2009; Ou et al., 2010), electrochemical (Boon et al., 2003, 2000; Deng et al., 2009; Drummond et al., 2003; Kelley et al., 1997; Liu and Lin, 2007; Ostatná et al., 2005; Polsky et al., 2006; Wang et al., 2001; Wong and Gooding, 2006), quartz crystal microbalance (Lazerges et al., 2006) and conductometric techniques (Sergeyeva et al., 1999). Recently electrochemical sensing becomes popular for its simplicity, accuracy and inexpensively (Mehrgardi and Daneshtalab, 2011; Tanaka et al., 2010).

The idea that the π-stack in DNA might serve a good pathway for charge transfer (CT), was suggested half century ago (Eley and Spivey, 1962). The small perturbation in the π-stack of DNA sequence causes a dramatic effect on the charge transfer in DNA duplex; therefore the detection of mutation, base lesions and protein binding could be explored by monitoring of CT in DNA (Gorodetsky et al., 2008a). The ability of CT in DNA duplexes vs. single strand is a good concept to a variety of fields including spectroscopy (Buzzeo and Barton, 2008; Kelley et al., 1999), conductivity measurement (Kodama et al., 2009), medical research (Chen et al., 2008) and the construction of DNA biosensors (Buzzeo and Barton, 2008; Kelley and Barton, 1999) as well. Barton and her co-workers are pioneers in the CT-based DNA hybridization biosensors and they used redox reporter such as Redmond red (Buzzeo and Barton, 2008), daunomycin (Kelley et al., 1999) and methylene blue (Kelley et al., 1997). Different types of SBM such as C–A, C–T, G–A, G–T, T–T, C–C, G–G and A–A can be appeared in the DNA sequences. C–T, C–A, T–T, G–G and A mismatches diminish the CT significantly. However, thermodynamically stable mismatches such as G–A and G–T mismatches do not affect on the charge transfer dramatically (Boon et al., 2000; Gorodetsky et al., 2008a); therefore for their detection need to enhance the sensitivity of the assays. There are several methods for amplification of signals such as electrocatalytic amplification (Boon et al., 2003, 2000), bioelectrocatalysis using enzymatic assays (Patolsky et al., 1999; Willner et al., 2009), covalent binding of redox reporters on the top of target DNA (Gorodetsky et al., 2008b), sensitive enhancement using negative intercalators (Mearns et al., 2006; Mehrgardi and Daneshtalab, 2011) and signal amplification using metal nanoparticles (Fang et al., 2008; Li et al., 2010). Among of these protocols, metal nanoparticles offer excellent prospects for chemical and biological sensing. Especially nanoparticle based biosensors offer excellent prospects for hybridization detection assays. Gold nanoparticles as oligonucleotide labels in DNA hybridization detection were used

* Corresponding author. Tel.: +98 311 7932710; fax: +98 311 6689732.
E-mail addresses: m.mehrgardi@sci.ui.ac.ir, m.mehrgardi@gmail.com (M.A. Mehrgardi).

0956-5663/$ – see front matter © 2011 Elsevier B.V. All rights reserved.
doi:10.1016/j.bios.2011.04.020

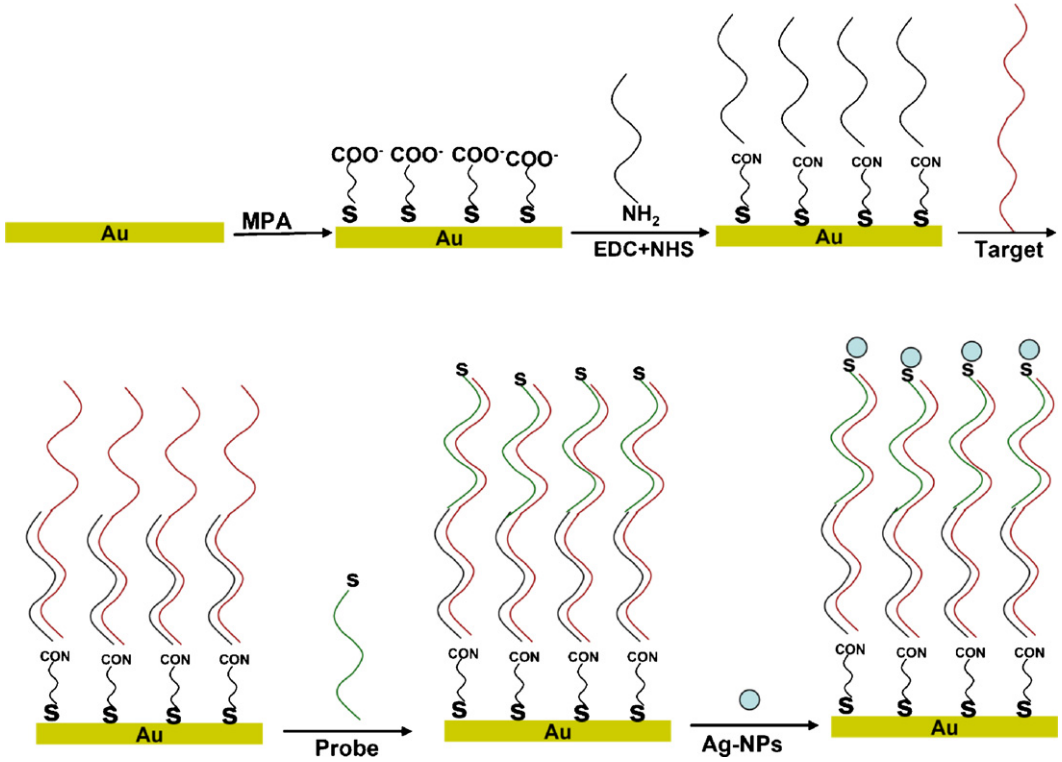

Scheme 1. Schematic plan of modification of electrode surface.

by several groups (Fang et al., 2008; Li et al., 2010; Wang et al., 2001). Mirkin and co-workers have developed DNA sensors using hybridization-induced changes in (distance-dependent) optical properties of gold-particle-modified oligonucleotide (Elghanian et al., 1997). Also, oligonucleotide-functionalized Au-nanoparticles following silver deposition on gold nanoparticles was used by the same group (Storhoff et al., 1998) in histochemical electromicroscopy visualization of protein–antibody and DNA–conjugated. Also silver enhanced gold nanoparticles were used in different way (Cai et al., 2002a,b). In these works gold nanoparticles were attached to the end of oligonucleotide and silver was deposited on the gold nanoparticles and then the stripping oxidation signal of silver was followed as an analytical signal (Cai et al., 2002a). Also, silver nanoparticles were used as oligonucleotide labeling tags by Cai group. Consequently, the nanoparticles were dissolved and silver ions were determined by anodic stripping voltammetry (Cai et al., 2002b).

In the present study, Ag-NPs have been used as redox reporters directly. The differential pulse voltammetric responses of oxidation of Ag-NPs are used to detect target hybridization. The integrity of base staking is necessary for efficient long-rang charge transfer (LCT) in DNA through the staking of bases (Kelley et al., 1997). The presence of a SBM shuts down the charge transfer and so Ag-NPs cannot be oxidized.

2. Experimental

2.1. Materials

N-hydroxylsuccinimide (NHS), N-(3-dimethylaminopropyl)-n-ethyl carbodimide hydrochloride (EDC), 3-mercaptopropionic acid (MPA), potassium ferrocyanide, potassium ferricyanide, nitric acid, sulfuric acid, acetic acid, sodium dihydrogen phosphate, disodium hydrogen phosphate, sodium chloride, magnesium chloride, sodium borohydride, sodium citrate tri-hydrate and silver nitrate were purchased from commercial sources (Merck or Sigma) and used as received, without further purification. The distilled-deionized water was used in all solution preparation (18 MΩ).

The stock solution of the oligonucleotides (2 μM) were prepared with PBS buffer solution and kept frozen at −20 °C. All experiment was performed at room temperature in a three-electrode electrochemical cell. In this study, DNA oligonucleotides were obtained from Eurofins MWG/Operon Co. and had the following sequence (From 5′ to 3′):

Probe:	HS-TCACTGCAAA
Capture:	CTCATGGTCC-NH_2
Complementary:	GGACCATGAGTTTGCAGTGA
NON-complementary:	ATCTACTACTGCATTCCGTC
G–A mismatch:	Near:GGAC<u>A</u>ATGAGTTTGCAGTGA
	Far: GGACCATGAGTTTGCAG<u>G</u>GA
G–T mismatch:	Near: GGACC<u>G</u>TGAGTTTGCAGTGA
	Far: GGACCATGAGTTTGC<u>G</u>GTGA
C–A mismatch:	Near:GGACCA<u>C</u>GAGTTTGCAGTGA
	Far: GGACCATGAGTTTGCAG<u>C</u>GA
T–T mismatch:	Near: GGACC<u>T</u>TGAGTTTGCAGTGA
	Far: GGACCATGAGTTTGC<u>T</u>GTGA

Electrochemical experiments were carried out using an Autolab electrochemical system PGSTAT 30 [ECO CHEMIE, The Netherlands] driven by GPES software. A conventional three-electrode system, consisting small parts of gold recordable compact disks (CD-R) as working electrode, a platinum wire as an auxiliary electrode and an Ag/AgCl/3.0 M KCl reference electrode was used for experiments. The differential pulse voltammograms have been recorded at the scan rate of 20 mV s^{-1} and the pulse amplitude of 25 mV. EIS experiments were accomplished at open circuit potential (O.C.P.) as constant DC potential. The applied AC potential was 5 mV.

2.2. Preparation of the Ag-NPs

Ag-NPs were prepared by the chemical reduction of Ag^+ ions in the presence of the $NaBH_4$ according previously reported procedure (Mulfinger et al., 2007; Wang et al., 1998). Briefly, 10.00 mL

silver nitrate solution (1.0 mM) was added drop by drop to 30.00 mL aliquot of 2.0 mM $NaBH_4$ at 0 °C until the solution turns to light yellow. Then 50.0 mg of sodium citrate tri-hydrate was added to the solution as a stabilizer reagent to prevent the aggregation of Ag-NPs. The colloid was continuously stirred while it was allowed to warm to room temperature. Ag-NPs could be stored in dark bottle (4 °C) for several days. TEM image of the nanoparticles has been presented in Fig. S1 (Supplementary Material). As Fig. S1 shows the average size of Ag-NPs is roughly 10 ± 3 nm.

2.3. Electrode modification and DNA hybridization detection

The gold electrode was prepared from a recordable compact disk according to previously published method (Angnes et al., 2000; Kiani and Fard, 2009). Briefly, a piece CD was cut and the protective layer was removed by putting it in the concentrated HNO_3. Then it was washed with water thoroughly. Now the gold surface is exposed and it could be used as a working electrode. The surface area of the gold electrode was measured by following its voltammogram in 0.5 M of sulfuric acid and assuming that a specific charge of 386 μC $cm^{-2}$is required for gold oxide reduction (Kiani and Fard, 2009). The surface area of the gold electrode was obtained equal to 0.22 ± 0.02 cm^2.

Scheme 1 shows the different modification steps of the gold electrode. The gold piece was secured to the bottom of a Teflon cell with an O-ring. In first step of the modification, a layer of 3-mercaptopropionic acid (MPA) was self-assembled on the surface of Au electrode. In this step, 2 mL of 50 mM aqueous solution of MPA was placed on the electrode surface overnight. After washing the electrode, the carboxylic groups on the surface was activated using 20 mM EDC solution and 30 mM NHS in phosphate buffer (pH 5.5) for 2 h. The electrode was then washed and 12 μL amine-labeled of capture DNA was dropped on the electrode and wait 2 h until the covalent bond between activated carboxylic groups and amino label of capture DNA is formed. Then the electrode surface was washed with 0.05 M phosphate buffer (pH 7.4). In the next step, 12 μL of target DNA was placed on the electrode for 20 min that a part of target is hybridized with capture. Next, 15 μL of deprotected thiolated-DNA probe, was dropped on the electrode surface for 2 h. The probe is complementary with non-hybridized section of the target and would be hybridized with this part. Each step of modification was monitored by EIS. For EIS analysis a solution of 0.5 mM potassium ferricyanide and potassium ferrocyanide (1:1) in 0.1 M KCl and 0.02 M of phosphate buffer with pH 5.5 was used. The optimum times for different steps has been obtained using this technique. In the last step of the electrode modification, 40 μL of Ag-NP solution and 40 μL of 1 M phosphate buffer with pH 5 were placed on electrode surface for 8 hours.

Differential pulse voltammetry (DPV) was used to electrochemical detection of SBMs. 3 mL of 0.15 M phosphate buffer (pH 5.5) was placed into the Teflon cell, containing the modified Au electrode, then DPV determination of Ag-NPs attached on DNA probe was performed in a scan from −0.2 to +0.55 V.

3. Results and discussion

As it was mentioned in the introduction section, the single base mismatches perturb the π-stack of DNA; therefore shut down the CT through DNA. There are two main problems in the most of electrochemical DNA hybridization biosensors based on the CT when the redox reporters are used in the solution: (a) direct electron transfer of redox reporter with the electrode surface via pinholes of recognition layer and (b) positioning of the reporter before the SBM in DNA duplexes (Ahangar and Mehrgardi, 2011; Mehrgardi and Daneshtalab, 2011). In the present assay, the Ag-NPs are immobilized on the top of the oligonucleotide in fixed positions and cannot be oxidized on the electrode surface directly or take place before the mismatch position. So the sensitivity of the biosensor has been improved and the biosensor is capable to discriminate different types of SMBs including thermodynamically stable ones. In this method the electrode are stable and it can be use for several times, but in previous work in the stripping step the electrode and DNA layer were destroyed.

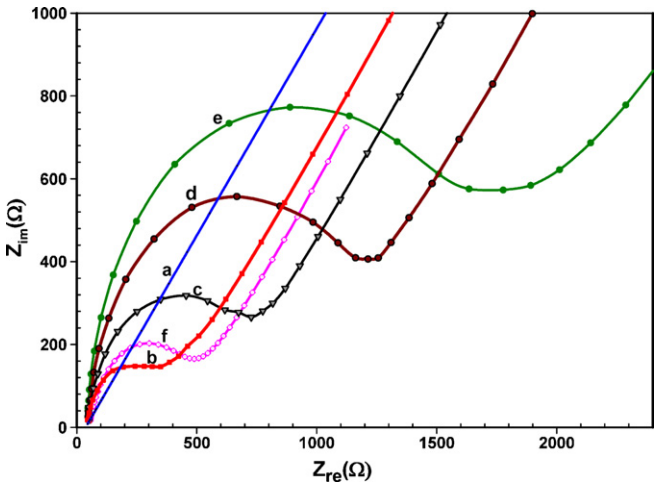

Fig. 1. EIS measurements were performed in $[Fe(CN)_6^{3-/4-}]$ (5×10^{-4} M; 1:1) as a negatively charged redox probe, at O.C.P. asa constant DC potential on (a) bare Au, (b) MPA self assembly, (c) after capture immobilization, (d) target hybridization, (e) probe hybridization and (f) Ag-NPs modification.

3.1. EIS behavior of electrode surface in modification steps

EIS is an effective method for the surface analysis and the investigation of self-assembled monolayers (SAMs). An important advantage of EIS is that does not damage the biomolecular layer on the electrode surface. Binding of biomaterial on electrode surface decrease the double-layer capacitance and retards the interfacial electron-transfer kinetics (Daniels and Pourmand, 2007). These effects depend on the molecular and immobilization characteristics of the deposited film on the surface. Fig. 1 shows the impedance features of the electrode interfaces upon the different steps of the modification. The electron transfer kinetics of $[Fe(CN)_6]^{3-/4-}$ specially on the short chain (MPA) that was used in this work is very fast (Shervedani and Pourbeyram, 2009); therefore, the electron transfer resistance (R_{ct}) reach to 420 Ω (Fig. 1b). Upon the covalent binding of the DNA capture, hybridization with complementary target and then hybridization with probe DNA (Fig. 1c, d and e, respectively), the electron transfer resistance (R_{ct}) increase. This change stemming from the blocking of the electrode surface and electrostatic repulsion of $[Fe(CN)_6]^{3-/4-}$ probe due to negative charge of DNA. In the final step of modification Ag-NPs are connected to the thiol group of the probe DNA. By immobilization of Ag-NPs on the top of the DNA, the electrochemical would occur on the surface of Ag-NPs via charge transfer through DNA and it would improve the kinetics and diminish R_{ct}. This is in consistence with previously published reports (Fu et al., 2005; Li et al., 2009; Liang et al., 2009).

3.2. Quantitation of surface density of DNA immobilization

The coverage of DNA immobilization at the electrode surface can be estimated using the number of cationic redox molecules that electrostatically associated to the anionic phosphate backbone of DNA (Steel et al., 1998). Briefly, after the immobilization of DNA

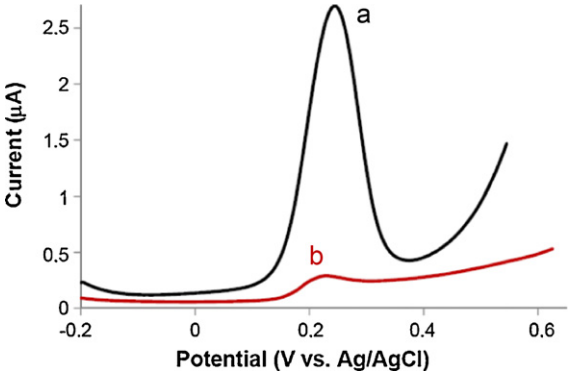

Fig. 2. Differential pulse voltammograms of the biosensor by hybridizing with (a) complementary target and (b) non-complementary target.

on the electrode surface, the modified electrode was placed in hexaamine ruthenium (III)(RuHex) solution with low ionic strength (0.05 M KCl). Then the amount of cationic redox marker, RuHex, was measured by chronocoulometry. Using the Cottrell equation, the chronocoulometric intercept at $t = 0$ is sum of the double layer charging and the surface surplus terms. The surface surplus terms are determined by the difference between the chronocoulometric intercepts for the identical potential step experiment in the presence and absence of redox marker. By following the relationship of the saturated surface surplus of RuHex in converted to DNA surface density: $\Gamma_{DNA} = \Gamma_0(z/m)(NA)$

where Γ_{DNA} is the probe surface density in molecules/cm^2, m is the number of bases in probe DNA, z is the charge of RuHex and N_A is Avogadro's number. At last the surface density of probe DNA has been obtained equal to $4.4 \pm 0.4 \times 10^{12}$ molecules cm^{-2}.

3.3. Voltammetric transductions

The ability of DNA recognition layer to charge transfer has been monitored by following the oxidation signal of immobilized Ag-NPs on the top of monolayer. The different double stranded structures of DNA in the recognition layer formed by the complementary target, targets containing single base mismatches and non-complementary target as well show different charge transfer kinetics; therefore different oxidation currents. Fig. S2 (Supplementary Material) shows the DPV of Ag-NPs solution containing 0.1 M phosphate buffer on the bare gold electrode. In the preliminary experiments, the capability of the biosensor for discrimination between complementary and non-complementary targets was checked by differential pulse voltammetry as presented in Fig. 2a and b. The formed ds-DNA on the surface of the electrode by hybridizing of probe and capture DNA with complementary target is a good path for charge transfer; therefore a well-defined oxidation peak for Ag-NPs is appeared around 0.24 V (Fig. 2a), while the signal of the assay for non-complementary target is very weak (8% of the signal for complementary target, Fig. 2b). It would be expected that the non-complementary targets do not hybridize with the capture and probe DNA; therefore no signal is observed. However, some Ag-NPs could be physically adsorbed on the recognition layer and produce signal. Fortunately it is extremely lower than the obtained signals from the complementary targets.

The analytical performance of the biosensor was explored using the different amounts of the complementary target in a 12 μL aliquot of the target solution according to the described procedure. The relationship between peak current of Ag-NPs oxidation and the logarithm of the amount of target is described in the Fig. 3. The anodic peak currents of electrochemical oxidation of Ag-NPs are increased by the increase of the complementary target amounts up to 16 pmol and then the signal remain constant roughly. Also the

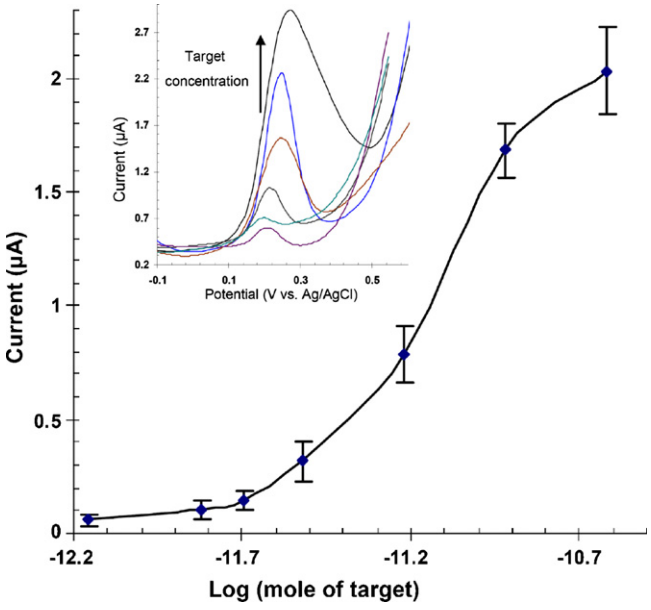

Fig. 3. Differential pulse voltammogram of different amounts of complementary DNA vs. logarithm of their amounts in mole. Inset shows voltammograms for different amounts.

experiments demonstrate that the assay can detect sub-picomoles of the target

In some other experiments, the effect of single base mismatches and their positions in the double stranded structure on the oxidation signal of Ag-NPs and the capability of the assay for detection of the mismatches were investigated. Fig. S3 (Supplementary Material) compares the voltammograms for complementary, non-complementary and different targets containing various mismatches including G–A, G–T, C–A and T–T in the far and near positions relative to the electrode surface. As the voltammograms show, the presence of a single base mismatch in the structure of the targets even thermodynamically stable ones diminishes the oxidation signal of Ag-NPs dramatically, probably due to the perturbation in the π-stack of DNA and its charge transfer. Therefore by this strategy SBM can be detected easily. As it was mentioned in our recently published manuscripts (Ahangar and Mehrgardi, 2011; Mehrgardi and Daneshtalab, 2011), when the electrochemical reporter molecules are in the solution, they can penetrate through the DNA film or bind to a position before the mismatch. If it occurs, then the mismatches and perturbation in the π-stack, would not affect on the charge transfer from the electrode surface to the reporter.

It could be concluded that the observed signal is consisted by three different pathways: (a) charge transfer to the reporters that bind to the top of DNA and after mismatch position; (b) charge transfer to the reporters that penetrate through DNA film and bind to the position before the mismatch position and finally (c) direct charge transfer with the electrode surface through pinholes. It's obvious that the contributions of (a) and (b) are the same for complementary and mismatch targets. The ratio between curves b and c, for the far type and near type of the mismatches, are the same that this behavior confirms our hypothesis regarding covalently attached reporter at top of DNA reduces the charge transfer from pathway b. These parts of the signal reduce the sensitivity of the assay for discrimination of SBMs. However, it could be supposed that if the molecular reporters covalently attach on the top of DNA, it would not penetrate in DNA film and by fading the contribution of this part of the signal, the sensitivity of the biosensor is increased. To examine this hypothesis, the targets with the same mismatch types but at different positions have been designed and the signals

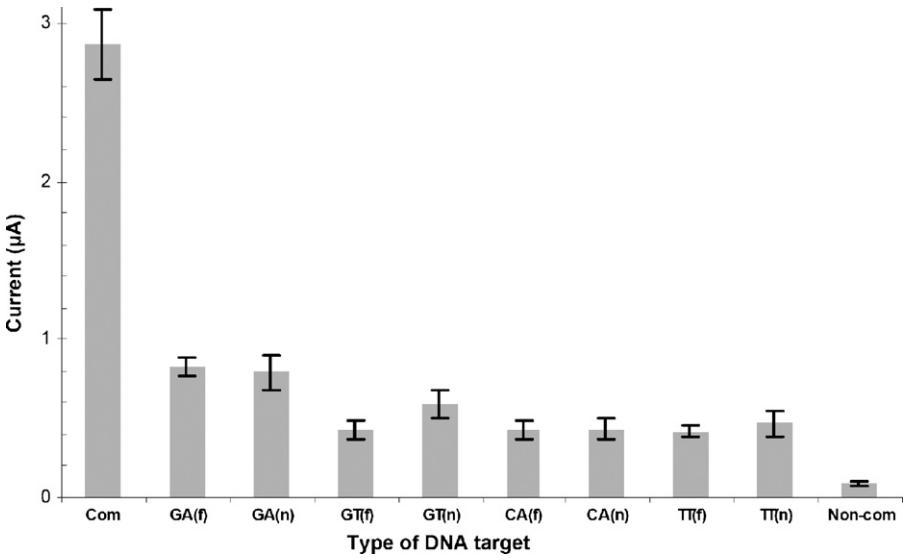

Fig. 4. The histogram of DPV signals for Ag-NPs modified electrode for different target.

Table 1
Comparison between the proposed assay and other reported techniques for the mismatch detection.

Method	Analytical technique	Type of mismatch	% SBM Signal decrease	Ref.
Redox-active intercalator, anthraquinonemonosulfonic acid	Osteryoung square wave voltammetry	G–A, C–A	70% and 85%	Wong and Gooding (2006)
DNA-mediated electrochemistry of disulfides	Square wave voltammetry	C–A	65%	Gorodetsky and Barton (2007)
Nucleic acid-functionalized Pt nanoparticles	Linear sweep voltammograms	C–A	40%	Polsky et al. (2006)
Nanoporous gold electrode electrostatic reporter	Chronocoulometry	G–G	90%	Hu et al. (2008)
A cadmium phosphate-loaded apoferritin nanoparticle probe	Square-wave voltammogram	C–C	90%	Liu and Lin (2007)
groove binder molecule ($CuPcS_4$), as redox reporter	Differential pulse voltammetry	G–A, G–T, C–A, T–T (far and near type)	30%	Mehrgardi and Daneshtalab (2011)
Redox-active intercalator: methylene blue	Differential pulse voltammetry	G–U	45%	Ostatná et al. (2005)
DNA biosensor based on a silver nanoparticle label	Anodic stripping voltammetry	A–A	55%	Cai et al. (2002b)
This proposed assay	Differential pulse voltammetry	G–A, G–T, C–A, T–T (far and near)	71–89%	Present work

of Ag-NPs were monitored. As the figure shows, there are no significant differences between the far and near mismatched targets demonstrating that Ag-NPs are fixed on the top of DNA and do not penetrate in the film. Overall results for different targets are shown as some histograms in Fig. 4 demonstrating the capability of the assay for discrimination of complementary target from non complementary target and different types of SBMs as well.

3.4. EIS investigations

In the EIS analysis for sundry DNA targets, the charge transfer resistances have been used as the analytical signals. Fig. S4 (Supplementary Material) shows the Nyquist plots for different targets is shown in. Non-complementary target does not hybridize with the capture and probe DNA, so Ag-NPs would not attach on the modified electrode. Therefore it shows the biggest R_{ct} in compared to the other DNA targets ($R_{ct} = 900 \pm 59\ \Omega$). In contrast, the complementary target shows the smallest R_{ct} ($R_{ct} = 198 \pm 13\ \Omega$) due to the good base pair stacking and fast charge transfer through the formed double helix. Different targets containing various types of SBMs have Ag-NPs at the top of recognition layer on the electrode, but the presence of the SBMs perturb the π-stacks and charge transfer through DNA, so they could not mediate the charge to Ag-NPs and R_{ct} would be increased. In EIS analysis of various DNA target, the R_{ct} of Nyquist plot have significant distinction; so by EIS analysis of modified electrode with various target, SBM can be detected. However the differences of DPV signal is more efficient than EIS signals.

4. Conclusion

A new DNA hybridization biosensor for detection single base mismatches has been described in this manuscript. In Table 1, a comparison between previously reported assays as and the present biosensor is shown. In the most of the manuscripts, thermodynamically stable mismatches such as G–A and G–T mismatches were not investigated. The present assay shows acceptable performance and G–A and G–T mismatches could be detected simply.

By following the electrochemical oxidation signal of Ag-NPs and fading the direct oxidation of the redox reporter on the electrode surface, the signal amplification was achieved. This biosensor is able to distinguish between complementary, non-complementary target DNA and even targets with a single base mismatches; including the most thermodynamically stable G–A G–T mismatches. The direct detection of Ag-NPs target DNA tag decrease the problem of pinhole in DNA biosensor and the problem of positioning redox reporter before the SBM in DNA sequence. This biosensor by diminishing the effect of these problems in biosensors increased the difference between complementary target and one with SBM. Several types of mismatches such as C–A, T–T, G–T and G–T were detected using this method.

Acknowledgment

The Authors would like gratefully acknowledge the financial support of this project by research council of University of Isfahan under contract No. 10470/SZ89.

Appendix A. Supplementary data

Supplementary data associated with this article can be found, in the online version, at doi:10.1016/j.bios.2011.04.020.

References

Ahangar, L.E., Mehrgardi, M.A., 2011. Electrochim. Acta 56, 2725–2729.
Angnes, L., Richter, E.M., Augelli, M.A., Kume, G.H., 2000. Anal. Chem. 72, 5503–5506.
Boon, E.M., Ceres, D.M., Drummond, T.G., Hill, M.G., Barton, J.K., 2000. Nat. Biotechnol. 18, 1096–1100.
Boon, E.M., Barton, J.K., Bhagat, V., Nersissian, M., Wang, W., Hill, M.G., 2003. Langmuir 19, 9255–9259.
Buzzeo, M.C., Barton, J.K., 2008. Bioconjug. Chem. 19, 2110–2112.
Cai, H., Wang, Y., He, P., Fang, Y., 2002a. Anal. Chim. Acta 469, 165–172.
Cai, H., Xu, Y., Zhu, N., He, P., Fang, Y., 2002b. Analyst 127, 803–808.
Chen, J., Zhang, J., Wang, K., Huang, L., Lin, X., Chen, G., 2008. Electrochem. Commun. 10, 1448–1451.
Daniels, J., Pourmand, N., 2007. Electroanalysis 19, 1239–1257.
Deng, C., Chen, J., Nie, L., Nie, Z., Yao, S., 2009. Anal. Chem. 81, 9972–9978.
Drummond, T.G., Hill, M.G., Barton, J.K., 2003. Nat. Biotechnol. 21, 1192–1199.
Eley, D., Spivey, D., 1962. Trans. Faraday Soc. 58, 405–410.
Elghanian, R., Storhoff, J.J., Mucic, R.C., Letsinger, R.L., Mirkin, C.A., 1997. Science 277, 1078–1081.
Fang, C., Fan, Y., Kong, J., Gao, Z., Balasubramanian, N., 2008. Anal. Chem. 80, 9387–9394.
Fu, Y., Yuan, R., Xu, L., Chai, Y., Zhong, X., Tang, D., 2005. Biochem. Eng. J 23, 37–44.
Gorodetsky, A.A., Barton, J.K., 2007. J. Am. Chem. Soc. 129, 6074–6075.
Gorodetsky, A.A., Buzzeo, M.C., Barton, J.K., 2008a. Bioconjug. Chem. 19, 2285–2296.
Gorodetsky, A.A., Dietrich, L.E.P., Lee, P.E., Demple, B., Newman, D.K., Barton, J.K., 2008b. Proc. Acad. Sci. 105, 3684–3689.
Hu, K., Lan, D., Li, X., Zhang, S., 2008. Anal. Chem. 80, 9124–9130.
Kelley, S.O., Barton, J.K., 1999. Science 283, 375–381.
Kelley, S.O., Barton, J.K., Jackson, N.M., Hill, M.G., 1997. Bioconjug. Chem. 8, 31–37.
Kelley, S.O., Jackson, N.M., Hill, M.G., Barton, J.K., 1999. Angew. Chem. Int. Ed. 38, 941–945.
Kiani, A., Fard, E.N., 2009. Electrochim. Acta 54, 7254–7259.
Kodama, T., Jain, A., Goodson, K.E., 2009. Nano Lett. 9, 2005–2009.
Lazerges, M., Perrot, H., Zeghib, N., Antoine, E., Compere, C., 2006. Sens. Actuators B 120, 329–337.
Li, G., Li, X., Wan, J., Zhang, S., 2009. Biosens. Bioelectron. 24, 3281–3287.
Li, S., Li, X., Zhang, J., Zhang, Y., Han, J., Jiang, L., 2010. Colloids Surf. Physicochem. Eng. Aspects 364, 158–162.
Liang, W., Yi, W., Li, S., Yuan, R., Chen, A., Chen, S., Xiang, G., Hu, C., 2009. Clin. Biochem 42, 1524–1530.
Liu, G., Lin, Y., 2007. J. Am. Chem. Soc. 129, 10394–10401.
Mearns, F., Wong, E., Short, K., Hibbert, D., Gooding, J., 2006. Electroanalysis 18, 1971–1981.
Mehrgardi, M.A., Daneshtalab, R., 2011. J. Electroanal. Chem. 650, 214–218.
Mulfinger, L., Solomon, S.D., Bahadory, M., Jeyarajasingam, A.V., Rutkowsky, S.A., Boritz, C., 2007. J. Chem. Educ. 84, 322.
Niu, S.-y., Li, Q.-y., Ren, R., Zhang, S.-s., 2009. Biosens. Bioelectron. 24, 2943–2946.
Ostatná, V., Dolinnaya, N., Andreev, S., Oretskaya, T., Wang, J., Hianik, T., 2005. Bioelectrochemistry 67, 205–210.
Ou, L.-J., Jin, P.-Y., Chu, X., Jiang, J.-H., Yu, R.-Q., 2010. Anal. Chem. 82, 6015–6024.
Patolsky, F., Katz, E., Bardea, A., Willner, I., 1999. Langmuir 15, 3703–3706.
Polsky, R., Gill, R., Kaganovsky, L., Willner, I., 2006. Anal. Chem. 78, 2268–2271.
Sergeyeva, T.A., Piletsky, S.L., Panasyuk, T.L., El'skaya, A.V., Brovko, A.A., Slinchenko, E.A., Sergeeva, L.M., 1999. Analyst 124, 331–334.
Shervedani, R.K., Pourbeyram, S., 2009. Biosens. Bioelectron. 24, 2199–2204.
Steel, A.B., Herne, T.M., Tarlov, M.J., 1998. Anal. Chem. 70, 4670–4677.
Storhoff, J.J., Elghanian, R., Mucic, R.C., Mirkin, C.A., Letsinger, R.L., 1998. J. Am. Chem. Soc. 120, 1959–1964.
Tanaka, M., Elias, B., Barton, J.K., 2010. J. Org. Chem. 75, 2423–2428.
Wang, W., Efrima, S., Regev, O., 1998. Langmuir 14, 602–610.
Wang, J., Xu, D., Kawde, A.-N., Polsky, R., 2001. Anal. Chem. 73, 5576–5581.
Willner, I., Shlyahovsky, B., Willner, B., Zayats, M., 2009. In: Yingfu, L., Yi, L. (Eds.), Functional Nucleic Acids for Analytical Applications. Springer, New York, pp. 199–252.
Wong, E.L.S., Gooding, J.J., 2006. Anal. Chem. 78, 2138–2144.